sciendo

POLISH MARITIME RESEARCH 1 (113) 2022 Vol. 29; pp. 13-25
10.2478/pomr-2022-0002

DYNAMIC MOTIONS OF THE CABIN MOUNTED ON THE MONO-HULL PLANING BOAT USING SUSPENSION SYSTEM IN WAVES

Hassan Bahrami
Hassan Ghassemi*
Department of Maritime Engineering, Amirkabir University of Technology, Tehran, Iran

* Corresponding author: *gasemi@aut.ac.ir (H. Ghassemi)*

ABSTRACT

The necessity for higher speed and appropriate seakeeping performance of boats has led to extensive research. Hence, this research mainly discusses the optimal behavior of the boat against motions. From an economic point of view, reducing motions of the boat minimizes the damage caused by shock and vibration to the boat and equipment. Other benefits include comfort and safety and, as a result, improved human operating ability. Suspension systems are rarely used as motion controller in a boat. In multi-hull boats, the hull is an inseparable part of the vessels, so the wave will affect crew and equipment. This paper proposes and evaluates a novel concept boat equipped with a suspended cabin. The hull and superstructure (cabin) are separated in this new form by a simple passive suspension system. This study used numerical analysis to examine the seakeeping performance of the planing boat Fridsma model equipped with a passive suspension system under regular wave conditions. The hydrodynamics of the planing hull were modeled using commercial software, STAR-CCM+. For simulation of the passive suspension system between boat and cabin, MATLAB software was used. Results showed that the motion of the cabin, which is where the crew and equipment are located, decreased in regular waves.

Keywords: Planing hull, Fridsma model, Cabin, Suspension system, Dynamic motions, Wave effect.

INTRODUCTION

Improving ride comfort is a significant issue in the transportation industry, so much research and development have been done on this subject. For road vehicles, one of the most widely used reliable methods is suspension techniques, which typically include springs, dampers, tires, and a set of linkages. The suspension system provides a specific reduction of vibration oscillations induced by road bumps resulting in improved ride comfort for vessels. The system puts designers and researchers in so many challenges. In comparison, a wave profile is more complex than a road profile in terms of magnitude and frequency of surface elevation. According to methods adopted, ride comfort and convenience of occupants of vessels can be done in three ways: roll stabilizing fin, shifting mass, and multi-body. [1]. A roll stabilizing fin is a protrusion from the ship's bottom surface used to minimize ship's roll. The most commonly used equipment in this category is bilge keels, fin-roll stabilizers, and rudder roll stabilizers. Shifting mass is a way of generating a reciprocal moment to lessen the motion of a ship's roll. Some tools include anti-roll tanks, mass dampers, and vertical weight stabilizers. Multi-body ship is the last approach. A multi-hull ship typically consists of a cabin part, a hull part, and a connecting part. The dynamic motion of the cabin and body can be discussed separately due to the expansion and contraction motion of the connecting components.

Rarely a calm sea can be found without waves. Sea is rough and gives significant motions to vessel's structure. Motions on

the boat have destructive effects on equipment and staffing, to control these effects, there must be sufficient knowledge of the motions on the vessel. A seakeeping test is used to determine the motions on the model boat.

Takahashi (1986) [2], proposed and tested a hydraulic support system designed to control the vertical motion called the Hi-Stable Cabin Craft (HSCC). The roll and pitch motions of the cabin relative to the body might be greatly decreased, according to the model scale test. Kihara et al. (1990) [3], built a full-scale twin-hull vessel, namely HSCC VOYAGER, tested it at sea trail, reducing the cabin roll and pitch by about 75% compared to the hull. A. Kükner et al. (1995) [4], investigated the dynamic motions of ships by examining experimental seakeeping in design and they took steps to increase human safety and reduce motions of the boat. The main focus of their research work was on the type of motions, vertical and lateral accelerations. S. M. Cook et al. (1999) [5], at the Research Center of the Curtin University studied the motions of heave and pitch of the boat in regular waves. Lu [6], in 2010 an MCS catamaran towing tank test using a suspension system, which consisted of a spring and an oil damper fitted between cabin and hull, found that dampers were firmer but had a more negligible effect on it has a cabin. Tsukamoto (2012) [7], showed that cabin's reduction of heave and pitch motion during towing with a towing speed of 1.5 m/s is improved by increasing damping coefficient and also showed that displacement between cabin and body can provide sufficient kinetic energy for reuse it. In 2012, Velodyne Marine [8], tested a multi-hull catamaran in California. The ship was equipped with a fully active suspension, which included advanced actuators and air suspensions. Low cabin oscillation was observed at high forward speeds along the sea trail. In Australia, Nauti Craft (2003–2021) [9], installed a hydraulic system in a suspended cabin catamaran. A sea trial of the full-scale ship showed a high level of suspended cabin ride comfort. Manhar et al. (2013) [10], [11], from the University of Florida, investigated the performance of seakeeping of WAN-V autonomous vessels with suspension, then results showed that the suspension system minimized heave motions of the boat's cabin. Jialin Han et al. (2015) [12],[13],[14] performed an experimental test of a catamaran model with suspension in waves. He evaluated its motion responses in varied heave, pitch, and roll motions under five control algorithms at two different speeds, compared to a fixed body catamaran under test conditions. They showed the motions were damped to a maximum of 93, an average of 74.8 percent.

This paper proposes and evaluates a novel concept boat equipped with a suspended cabin. The hull and superstructure (cabin) are separated in this new form by a simple passive suspension system. Due to the new design, it is necessary to know its dynamic performance. Heave and pitch motions are the essential dynamic motions of the boat that affect the equipment and will considerably impact the crew's performance. For this purpose, this study analyzed the seakeeping performance of the boat Fridsma model equipped with a passive suspension system under regular wave conditions using a numerical method.

NUMERICAL SIMULATION METHOD

In this study, the hydrodynamics of the planing hull were modeled using commercial software, STAR-CCM+. An implicit unsteady solver was used based on URANS with turbulence model. A Semi- Implicit Method for Pressure-Linked Equations (SIMPLE) has been used to solve the fluid field around the body. The Volume of Fluid (VOF) technique, which tracks the free surface boundary, was used to solve the two-phase flow combining air and water. The dynamic fluid-body interaction (DFBI) model in the code was activated to have 2DOF for the hull.

GOVERNING EQUATIONS OF FLUID

The homogenous multiphase Eulerian fluid approach is adopted in the current study to describe the interface between water and air mathematically. Both air and water share the same characteristics (in the free surface) such as velocity, turbulence, etc. The governing equations that need to be solved are the mass continuity equation, which is given as [15]:

$$\frac{\partial}{\partial x_i}(\rho u_i) = 0 \tag{1}$$

The momentum equations, which are given as:

$$\frac{\partial}{\partial x_i}(\rho u_i u_j) = -\frac{\partial \rho}{\partial x_i} + \frac{\partial}{\partial x_j}\left(-\rho\overline{u_i' u_j'}\right) + \frac{\partial}{\partial x_j}\left[\mu\left(\frac{\partial u_i}{\partial x_j} + \frac{\partial u_j}{\partial x_i} - \frac{2}{3}\delta_{ij}\frac{\partial u_l}{\partial x_l}\right)\right] \tag{2}$$

In order to capture the sharp interface of the free surface of the air-water boundary, the volume of fluid method is implemented. A transport equation (i.e. Eq. (3)) is then solved for the advection of this scalar quantity, using the velocity field obtained from the solution of the Navier-Stokes equations at the last time step.

$$\frac{\partial q}{\partial t} + \nabla \cdot (qu) = 0 \tag{3}$$

Numerical solution of Eq. (3) gives the volume fraction, q, for each phase (i.e., air and water) in all computational cells where $\sum_{k=1}^{2} q_k = 1$.

Furthermore, a k-ε turbulence model is applied to consider the viscous effects, which are expressed as follows:

$$\frac{\partial k_i}{\partial x_j} = \frac{\partial}{\partial x_i}\left[\left(\mu + \frac{\mu_t}{\sigma_k}\right)\frac{\partial k}{\partial x_i}\right] + G_k + G_b - \rho\varepsilon \tag{4}$$

$$\rho u_j \frac{\partial \varepsilon_i}{\partial x_i} = \frac{\partial}{\partial x_i}\left[\left(\mu + \frac{\mu_t}{\sigma_\varepsilon}\right)\frac{\partial \varepsilon}{\partial x_i}\right] + C_{l\varepsilon}\frac{\varepsilon}{k}\left(G_k + G_{3\varepsilon}G_b\right) - C_{2\varepsilon}\rho\frac{\varepsilon^2}{k} \tag{5}$$

where k is the turbulent kinetic energy and ε is the dissipation rate of the turbulent energy. Also, the parameters of and are the generation of turbulent kinetic energy due to the mean velocity gradients and buoyancy. Constant parameters of δ_ε, δ_k, $C_{l\varepsilon}$ and $C_{2\varepsilon}$ are the model constants and must be determined experimentally. On the other hand, μ_t and μ are also the turbulent eddy viscosity and the molecular dynamic viscosity, respectively.

Definition of Free Surface

The VOF method is adopted to capture the free surface. For a given computational domain V, Fluid 1 is in domain V_1, and Fluid 2 is in domain V_2. The function is defined as follows [16]:

$$\alpha(x, t) = \begin{cases} 1, x \in V_1 \\ 0, x \in V_2 \end{cases} \quad (6)$$

For a flow field composed of two incompatible fluids, α (x, t) is in accordance with:

$$\frac{\partial \alpha}{\partial t} + U.\nabla\alpha = 0 \quad (7)$$

where U = (u, v, w) is the fluid velocity field, and the VOF function is defined as the integral in the grid unit of α (x, t) divided by unit volume, i.e.,

$$C_{ijk} = \frac{1}{\Delta V_{ijk}} \int_{I_{ijk}} \alpha\,(x.t)dV \quad (8)$$

C_{ijk} is in accord with $(\partial C/\partial t) + U.\nabla C = 0$. When C=1, the grid is filled with Fluid 1. When C=0, the grid excludes Fluid 1. When 0<C<1, the grid contains free surface.

Generating Wave Method

The wave module of CFD software STAR-CCM+ is used to generate regular sinusoidal propagating waves in an infinite water depth. According to linear theory, the x and z-components of the velocity are given by the following equations [15].

$$v_x = \omega\zeta_a e^{kz} \sin(\omega t - kx) \quad (9)$$

$$v_z = \omega\zeta_a e^{kz} \cos(\omega t - kx) \quad (10)$$

$$\zeta = \zeta_a sin\,(\omega t - kx) \quad (11)$$

where:
ζ_a: wave amplitude,
$\omega=2\pi/T$: wave frequency,
$k=2\pi/\lambda$: wave number,
T: wave period,
λ: wavelength,
and *oxz* is the Cartesian coordinate at the free surface, which the x-axis is the direction of wave propagation and the z-axis is the positive when upward, with z = 0 the mean water level.

EQUATIONS OF MOTION (WITH SUSPENSION SYSTEM)

Schematic of a dynamic model of a boat with a suspension system and a free-body diagram of a two-body system is shown in Fig. 1. This computational model is commonly summarized into two cabin and boat (twin-hull) geometries coupled by two springs and dampers at the same distance from the cabin's center of gravity (CG) and the boat's center of gravity (Cg) at the front and rear. The geometry of the cabin is a rectangular cube, as shown in the Fig. 1 with the word Cabin. The boat and cabin are influenced by a moving force of a wave and hydrodynamic coefficients as well as a stiffness and damping of the suspension system. The damping coefficient with symbol C and the stiffness of the spring with symbol K for the suspension system is shown in the Fig. 1.

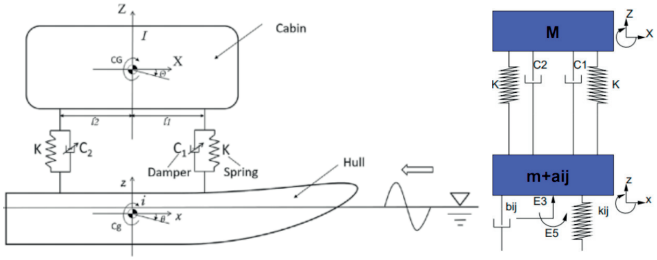

(a) (b)

Fig. 1. (a) schematic of a dynamic model of a boat with a suspension system [1](b) Free-body diagram of two body system

Due to the limited motions for model analysis to heave and pitch motions, four degrees of freedom have been considered to solve this simulation, which includes degrees of freedom:

- Z motion of the boat (Heave of the boat) (z)
- Z motion of the cabin (Heave of the cabin) (Z)
- Y Rotation of the boat (Pitch of the boat) (θ)
- Y Rotation of the cabin (Pitch of the cabin) (θ)

The changes of the cabin's transitional and rotational motions (heave and pitch) are considered around the cabin's center of mass (CG) and the boat's center of mass (Cg), respectively. Also, the coordinate system follows the right-hand rule. The equations of the motion at head waves can be expressed as [1]:

Heave of the Cabin:

$$M.\ddot{Z}(t) + C_1(t).\dot{Z}_{r1}(t) + C_2(t).\dot{Z}_{r2}(t) + K.[Z_{r1}(t) + Z_{r2}(t)] = 0 \quad (12)$$

Pitch of the Cabin:

$$I.\ddot{\theta}(t) + l_1.C_1(t).\dot{Z}_{r1}(t) + l_2.C_2(t).\dot{Z}_{r2}(t) + K.[\,l_1 Z_{r1}(t) + l_2 Z_{r2}(t)] = 0 \quad (13)$$

Heave of the Twin-hull:

$$(m + a_{33}).\ddot{z}(t) - C_1(t).\dot{Z}_{r1}(t) - C_2(t).\dot{Z}_{r2}(t) - K.[Z_{r1}(t) + Z_{r2}(t)] = E_3(t) - b_{33}\dot{z}(t) - k_{33}z(t) - a_{35}\ddot{\theta}(t) - b_{35}\dot{\theta}(t) - k_{35}\theta(t) \quad (14)$$

Pitch of the Twin-hull:

$$(i + a_{55}).\ddot{\theta}(t) - l_1C_1(t).\dot{Z}_{r1}(t) - l_2C_2(t).\dot{Z}_{r2}(t) - K.[l_1Z_{r1}(t) + l_2Z_{r2}(t)] = E_5(t) - b_{55}\dot{\theta}(t) - k_{55}\theta(t) - a_{53}\ddot{z}(t) - b_{53}\dot{z}(t) - k_{53}z(t) \quad (15)$$

where $Z_{r1}(t)$ and $Z_{r2}(t)$ represent the relative displacement of the front and rear suspension, respectively. They are written as:

$$Z_{r1}(t) = Z(t) - l_1\theta(t) - z(t) + l_1\theta(t) \quad (16)$$

$$Z_{r2}(t) = Z(t) + l_2\theta(t) - z(t) - l_2\theta(t) \quad (17)$$

The hydrodynamic forces and moments are calculated using STAR-CCM+. The hydrodynamic coefficients of the boat can be theoretically calculated by using the 2.5t theory and practical Savitsky's method. Because the solutions of response of the heave and pitch motions analysis shows that it is sensitive to the hydrodynamic coefficients, a more accurate method should be developed [17].

The matrix of equations is given as follows:

$$\begin{bmatrix} M & 0 & 0 & 0 \\ 0 & I & 0 & 0 \\ 0 & 0 & (m+a_{33}) & 0 \\ 0 & 0 & 0 & (i+a_{55}) \end{bmatrix} \begin{bmatrix} \ddot{Z} \\ \ddot{\theta} \\ \ddot{z} \\ \ddot{\theta} \end{bmatrix} + \begin{bmatrix} C_1 & C_2 & 0 & 0 \\ l_1C_1 & l_2C_2 & 0 & 0 \\ -C_1 & -C_2 & b_{33} & b_{35} \\ -l_1C_1 & -l_2C_2 & b_{53} & b_{55} \end{bmatrix} \begin{bmatrix} \dot{Z}_{r1} \\ \dot{Z}_{r2} \\ \dot{z} \\ \dot{\theta} \end{bmatrix} + \begin{bmatrix} K_1 & K_2 & 0 & 0 \\ l_1K_1 & l_2K_2 & 0 & 0 \\ -K_1 & -K_2 & k_{33} & k_{35} \\ -l_1K_1 & -l_2K_2 & k_{53} & k_{33} \end{bmatrix} \begin{bmatrix} Z_{r1} \\ Z_{r2} \\ z \\ \theta \end{bmatrix} = \begin{bmatrix} 0 \\ 0 \\ E_3 \\ E_5 \end{bmatrix} \quad (18)$$

The above parameters are given in nomenclature.

HULL DEFINITION

The Fridsma hull geometry definition is given in Fig. 2. The hull is comprised of idealized shapes: a bow consisting of four ruled surfaces followed by a wedge-shaped straight section with the constant deadrise angle of 20°. Fig. 2 shows the analytical formulas for the bounding curves of the ruled surfaces (A ruled surface can be described as the set of points swept by a moving straight line). The main particulars of model are given in Table 1.

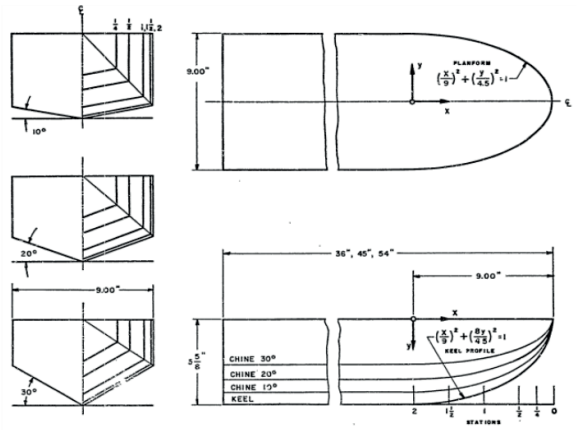

Fig. 2. The Fridsma hull geometry [18]

Tab. 1. Main particulars of the model and cabin

Symbol	Value	Definition
L	1.5 m	Length of the hull
L_c	1.23 m	Length of the cabin
b	0.3 m	Breadth of the hull
b_c	0.3 m	Breadth of the cabin
h	0.1875 m	Height of the hull
hc	0.05 m	Height of the cabin
m	16.40 kg	Mass of the hull
M	16.40 kg	Mass of the cabin
i	2.33 kg.m^2	Moment of inertia of the hull
I	2.07 kg.m^2	Moment of inertia of the cabin
X_{Cghull}	0.615 m (41%L)	longitudinal distance of center of gravity of the hull
$X_{Cgcabin}$	0.615 m	longitudinal distance of center of gravity of the cabin
Z_{cghull}	0.0882 m (0.294*b)	vertical distance of center of gravity of the hull
$Z_{cgcabin}$	0.5125 m	vertical distance of center of gravity of the cabin

MESH GENERATION

The domain dimensions were determined based on experience gained by ITTC on free surface flow hydrodynamic analyses [19]. The computational domain for simulation is approximately 4.5 m in front of the bow, 10 m aft, 1.5 m above deck, 3m below the keel, and 3m to the side of the boat. The velocity inlet is the boundary condition in front of the boat; the pressure outlet is the boundary condition behind the boat; the symmetry plane is the boundary condition of the center plane; and for the boat, no-slip wall boundary condition is used. Also, to prevent unnecessary calculations of the boundary layer's effects, the remaining sides were velocity inlets. All these boundary conditions are shown in Fig. 3.

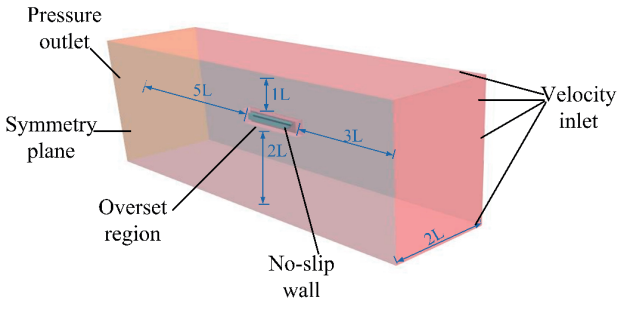

Fig. 3. Boundary conditions

The most challenging part of creating computation models is mesh generation. The quality of the mesh can influence both a correct solution and a duration of the solving time. The overset technique is used to model the boat dynamics. When dealing with moving bodies incorporating fluid-structure interaction, overset grid comes in useful. This grid implementation does

not require mesh change or deformation, which provides greater flexibility than conventional meshing techniques. Conservation of cell quality that should be considered at each time step is not an issue in overset grids, while this is one of the drawbacks of the deforming mesh when there are large body motions inside the flow [20]. There are a minimum of two zones in overset mesh issues. As shown in Fig. 4, one is background region, which includes the computational domain, and the other is a smaller region that consists of the moving body (Overset Region). Since the computational domain's dimensions are relatively large and the calculation is focused mainly on the flow field near the boat, the mesh near the boat is finer and gradually gets more and more sparse. The total number of cells is 856282.

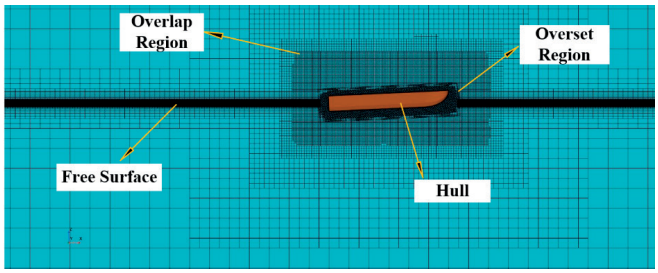

Fig. 4. Computational domain mesh

NUMERICAL RESULTS

In this part, we present our simulation results for the Fridsma hull and evaluate the effect of the suspension system on heave and pitch motions of the cabin in regular waves. The simulation was performed over 1000-time steps with a time-step size Δt=0.005s and 10 iterations per time step. The size of the time step was selected following the instructions provided by ITTC [19].

MESH INDEPENDENCY

To accurately describe the flow field and the force acting on the planing hull, very careful grid refinement is necessary in addition to the numerical model and boundary conditions. The intended value of wall Y plus can be used to compute the height of the first boundary layer grid. The value of wall Y plus is shown in Fig. 5, which is reasonable [21]. This could satisfy the turbulence equation's and wall function's requirements, and the flow of the boundary layer could be correctly simulated, ensuring its precision.

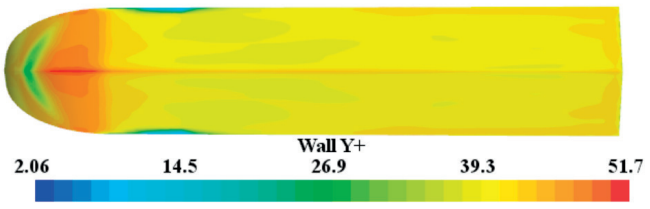

Fig. 5. Value of wall Y plus at Fr = 1.2

As a result, before presenting the main results, a mesh study was carried out to determine an optimum mesh size. For this purpose, different numbers of cells ranging from 500 thousand to 2 million cells are considered, and required simulations are performed. Fig. 6 shows the computed heave and pitch motion at Fr = 1.2, λ/L = 2 and H/b = 0.222 for each of these cases. This figure demonstrates that heave and pitch motions are different for the first mesh sizes, but they are roughly similar for the last three cases. As shown in Fig. 6, a medium-mesh (800 thousand cells) is suitable for the current issue.

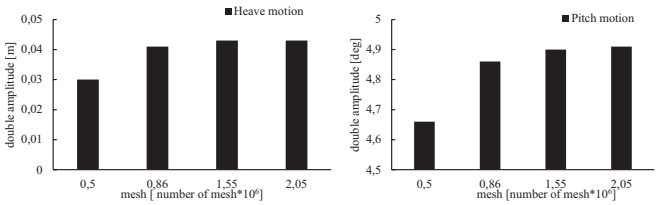

(a) *(b)*

Fig. 6. Mesh dependency at H/b=0.222 and λ/l=2 (Fr=1.2): (a) heave motion, (b) pitch motion

A verification study was carried out to demonstrate and ensure the method using the Grid Convergence Index (CGI), as shown in Table 2. This method is one of the most accurate methods for examining the meshing of simulations, which has been used in other articles [22]the ship bare hull case, the with-propeller case, and the with-propeller-and-duct case are also computed. Together, these computations provide for a -complete CFD comparison of the duct effects. Also, the Taguchi design of the experiment method is applied to investigate three parameters (angle of attack, trailing edge radius, and chord length. This study uses this method to calculate the discretization error estimation where the low percent of CGI is better for ensuring the solver. Celik presented this method in 2008. The reference [23]the Fluids Engineering Division of ASME has pursued activities concerning the detection, estimation and control of numerical uncertainty and/or error in computational fluid dynamics (CFD, has the details of this method's formulation. This report provides a quick overview of these parameters.

Tab. 2. Discretization error for Heave and Pitch based on grid convergence method at Fr=1.2, λ/L=2 and H/b=0.222

Parameter	Heave motion (m) (Double amplitude)	Pitch motion (deg) (Double amplitude)
N_0 (finer)	2045088	2045088
N_1 (fine)	1547025	1547025
N_2(medium)	856282	856282
N_3(course)	501203	501203
r_{21}	1.2179	1.2179
r_{32}	1.1955	1.1955
ϕ_0	0.043	4.91
ϕ_2	0.043	4.9
ϕ_3	0.041	4.86

Parameter	Heave motion (m) (Double amplitude)	Pitch motion (deg) (Double amplitude)
ϕ_4	0.03	4.66
s_a	9.7435	9.2222
e_a^{21}	4.6512	4.9078
e_{ext}^{21}	0.7917	0.1579
GCI_{fine}^{21}	0.99	0.20

In this method, apparent order s_a is expressed as:

$$s_a = \frac{1}{\ln(r_{21})}\left|\ln\left|\frac{\varepsilon_{32}}{\varepsilon_{21}}\right| + q(s_a)\right| \quad (19)$$

Auxiliary parameters are calculated as follows:

$$q(s_a) = \ln\left(\frac{r_{21}^{s_a} - s}{r_{32}^{s_a} - s}\right) \quad (20)$$

$$s = 1 \cdot sgn\left(\frac{\varepsilon_{32}}{\varepsilon_{21}}\right) \quad (21)$$

where, the refinement factors r for four different meshes, i.e. (0) finer, (1) fine, (2) medium, and (3) coarse, are $r_{21} = h_2/h_1$, $r_{32} = h_3/h_2$ (h_i is the average size of the mesh were determined from the number of the i-th mesh (N_i) and the calculating domain) that should be greater than 1.3. The parameter ε expresses as $\varepsilon_{32} = \phi_3 - \phi_2$, $\varepsilon_{21} = \phi_2 - \phi_1$ where ϕ_i denotes the solution (here Heave and Pitch) on the i-th mesh. Now, we can calculate the extrapolated value ϕ_{ext}, approximated relative error e_a, extrapolated relative error e_{ext}, and grid convergence index GCI_{medium} as follows:

$$\phi_{ext}^{21} = (r_{21}^{sa}\phi_1 - \phi_2)/(r_{21}^{s_a} - 1) \quad (22)$$

$$e_a^{21} = \left|\frac{\phi_1 - \phi_2}{\phi_1}\right| \quad (23)$$

$$e_{ext}^{21} = \left|\frac{\phi_{ext}^{21} - \phi_2}{\phi_{ext}^{21}}\right| \quad (24)$$

$$GCI_{medium}^{21} = \frac{1 \cdot 25e_a^{21}}{r_{21}^{s_a} - 1} \quad (25)$$

These parameters were calculated for heave and pitch values and are presented in Table 2. As can be seen from this table, the uncertainties values for heave and pitch were estimated "0.99%" and "0.2%", respectively.

VALIDATION

Fridsma tested his model boat in 1969 at Davidson Laboratory, and the results are publicly available [18]. He performed 16 test models with L/b values of 4, 5, and 6 at three deadrise angles in regular (1969) and irregular (1971) waves at three distinct speeds and three H/b ratios. Model A was used to compare heave and pitch motions at a regular wave in two different wave heights (H/b = 0.111 and 0.222) and varied wavelengths to Friedsma's experimental data [18]. Fig. 7 and 8 shows the comparison of RAOs between numerical results and experimental data under head waves at two values of H/b=0.111 and 0.222 and various λ/L. As observed in these figures, the calculated heave and pitch values were generally found in good agreement with the experimental data.

Also, Fig. 9 shows the comparison of time history between numerical results and experimental data in head waves at λ/L=4, H/b=0.222 and $\frac{V}{\sqrt{L}}$ = 6. The calculated heave and pitch motions were also in good agreement with experimental data in this state.

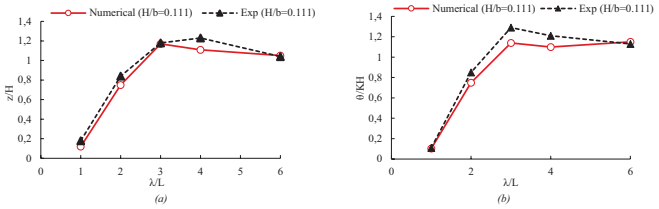

Fig. 7. Comparison of the RAOs between numerical results and experimental data against λ/L (Fr=1.2): (a) heave motion, (b) pitch motion

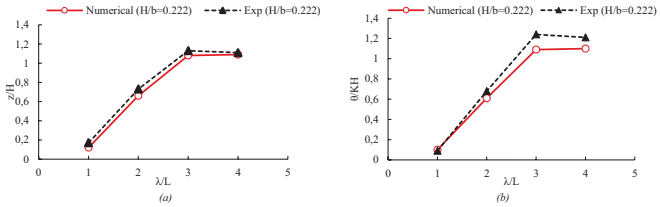

Fig. 8. Comparison of the RAOs between numerical results and experimental data against λ/L (Fr=1.2): (a) heave motion, (b) pitch motion

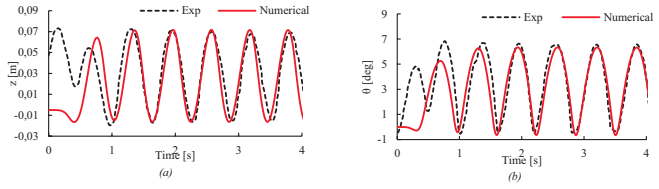

Fig. 9. Comparison of the time history between numerical results and experimental data at λ/L=4 and H/b=0.222 (: (a) heave motion, (b) pitch motion

FREE BODY SIMULATION (BARE HULL)

In this article, the dynamic motions of the boat and cabin are analyzed in three phases:

- Free body motion simulation (Bare hull)
- Boat with cabin (Rigid Mode) simulation
- Suspension system simulation

This part examines the boat without the cabin. The results obtained at two distinct wave heights (H/b =0.111, 0.222) and five various wavelengths (λ/L) are presented in Table 3. Fig. 10 shows the time history of heave and pitch motions of the bare hull at H/b = 0.222 and different wavelengths at Fr=1.2.

Tab. 3. Results of boat motions of bare hull in regular head wave at two distinct wave heights (H/b =0.111and 0.222) and five various wavelengths (Fr=1.2)

λ/L	H/b=0.111		H/b=0.222	
	Heave [m]	Pitch [deg]	Heave [m]	Pitch [deg]
1	0.004	0.82	0.008	1.59
2	0.025	2.99	0.044	4.88
3	0.039	3.07	0.072	5.81
4	0.037	2.20	0.073	4.39
6	0.035	1.53	0.072	2.82

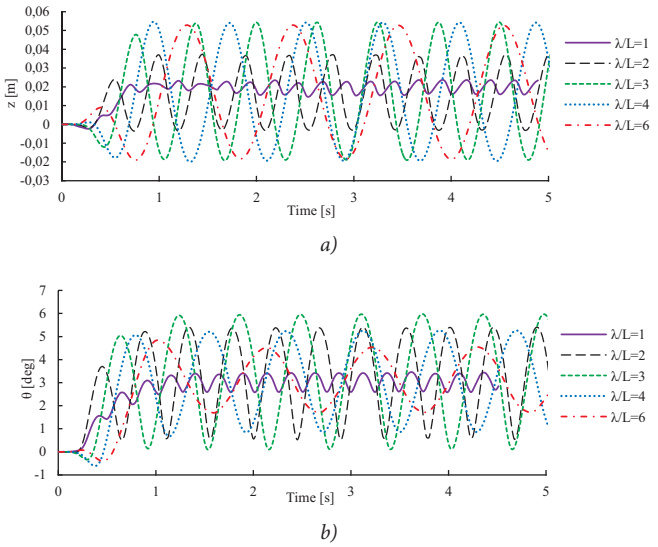

Fig. 10. Time histories of boat motions of bare hull in regular head waves at H/b =0.222 and different wavelengths (Fr=1.2): (a) heave motion, (b) pitch motion

BOAT WITH CABIN (RIGID MODE) SIMULATION

In Rigid mode, the cabin is positioned at a set distance on the top of the boat and is joined via a rigid body. The effects of the cabin's weight, moment, and center of gravity point on the boat's weight, moment, draft, and overall center of gravity are considered in this simulation.

In this part, the results are obtained at two distinct wave heights, (H/b =0.111 and 0.222), and five various wavelengths (λ/L) are presented in Table 4. Fig. 11 shows the time history of heave and pitch motions of the cabin for boat with cabin (Rigid Mode) at H/b = 0.222 and different wavelengths. Fig. 12 shows comparison of free surface elevation of the bare hull and boat with cabin (rigid mode) at H/b=0.222 and λ/L=2.

Tab. 4. Results of cabin motions of the model boat with cabin (Rigid Mode) motions in regular head waves at H/b =0.111-0.222 and different λ/L (Fr =1.2)

λ/L	H/b=0.111		H/b=0.222	
	Heave [m]	Pitch [deg]	Heave [m]	Pitch [deg]
1	0.004	0.64	0.007	1.19
2	0.014	2.04	0.027	3.68
3	0.039	3.81	0.069	6.61
4	0.045	3.32	0.091	6.63
6	0.039	1.91	0.081	3.86

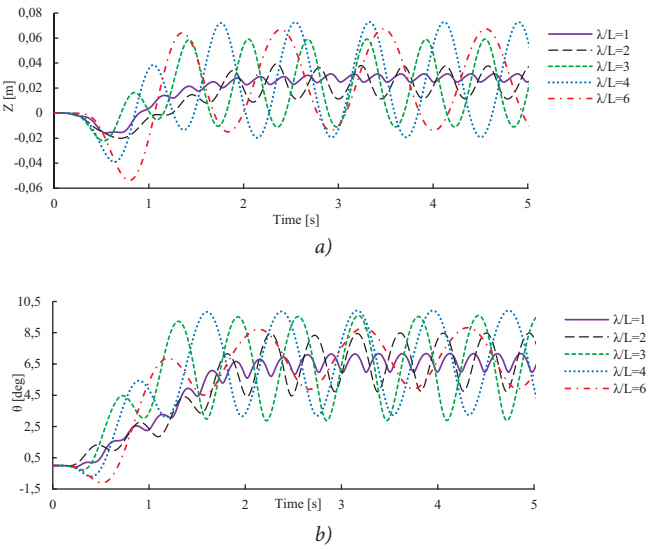

Fig. 11. Time histories of cabin motions of the model boat with cabin (Rigid Mode) in regular head waves at H/b =0.222 and different wavelengths (Fr=1.2): (a) heave motion, (b) pitch motion

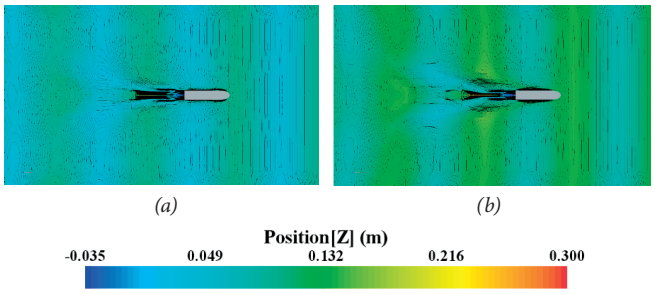

Fig. 12. Comparison of free surface elevation of the bare hull and boat with cabin at H/b=0.222 and λ/L=2 (Fr=1.2): (a)bare hull (b)with cabin

SUSPENSION SYSTEM SIMULATION

The dynamic model of the boat with a suspension system Fig. 1. This computational model comprises two parts a cabin and a boat hull. Geometries are coupled by two springs and dampers at the same distance from the cabin's center of gravity (CG) and the boat's center of gravity (Cg) at the front and rear. The geometry of the cabin is a rectangular cube, as shown in the Fig. 1 with the word Cabin. The boat and the cabin are influenced by moving forces of waves and hydrodynamic coefficients as well as the stiffness and damping of the suspension system. Due to the limited motions for model analysis to heave and pitch motions, four degrees of freedom have been considered to solve this simulation.

Equations 12~17 are the dynamic equations for coupling heave and pitch motions of the boat and cabin at head waves. By solving a system of differential equations (12~(17) simultaneously in MATLAB software, using the ODE45 function, the cabin motions can be obtained from excitation by the impact of wave force. Table 5 shows the input data and output results in MATLAB software.

Tab. 5. Input and Output parameters in MATLAB software

Input parameters		Output parameters	
Parameters Definition		Parameters	Definition
a_{ij}	Added mass ij, (i, j= 3-5)	Z	Displacement of the heave of the cabin
b_{ij}	Damping ij, (i, j= 3-5)	Z'_{cab}	Vertical velocity of the heave of the cabin
k_{ij}	Stiffness ij, (i, j= 3-5)	θ	Displacement of the pitch of the cabin
E_3 [N]	Wave exciting force	θ'_{cab}	Angular velocity of the pitch of the cabin
E_5 [N m]	Wave exciting moment	Z_{fore}	Relative displacement of the front suspension
M [kg]	Mass of the cabin	Z'_{fore}	Relative velocity of the front suspension
m [kg]	Mass of the hull	Z_{aft}	Relative displacement of the rear suspension
I [kg m^2]	Moment of inertia of the cabin	Z'_{aft}	Relative velocity of the rear suspension
i [kg m^2]	Moment of inertia of the hull	z	Displacement of the heave of the hull
l_1 [m]	Horizontal distance from front suspension to CG, Cg	z'_{hull}	Vertical velocity of the heave of the hull
l2 [m]	Horizontal distance from rear suspension to CG, Cg	θ	Displacement of the pitch of the hull
K [kg s^-2]	compression spring constant	θ'_{hull}	Angular velocity of the pitch of the hull
C_1 [kg s^-1]	Front damping coefficient		
C_2 [kg s^-1]	Rear damping coefficient		

The main specifications of the suspension system are given in Table 6. In this part, the results of the cabin motion obtained at two distinct wave heights (H/b =0.111, 0.222) and five various wavelengths (λ/L) are presented in Table 7. Fig. 13 shows the time history of the heave and pitch motions of the cabin and twin-hull for boat with cabin (suspension system) at H/b = 0.222 and different wavelengths (λ/L). It can be seen that the suspension system has significantly reduced the heave and the pitch motions of the cabin.

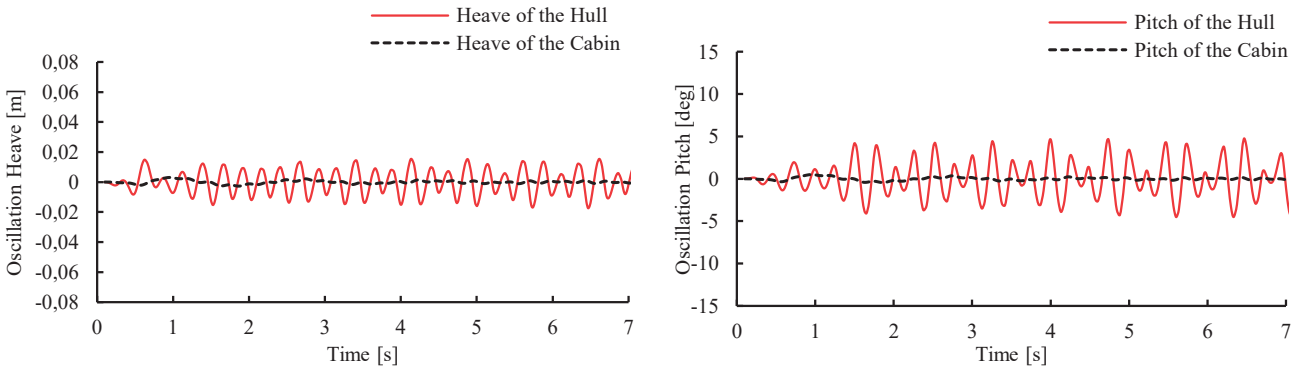

(a) λ/L=1

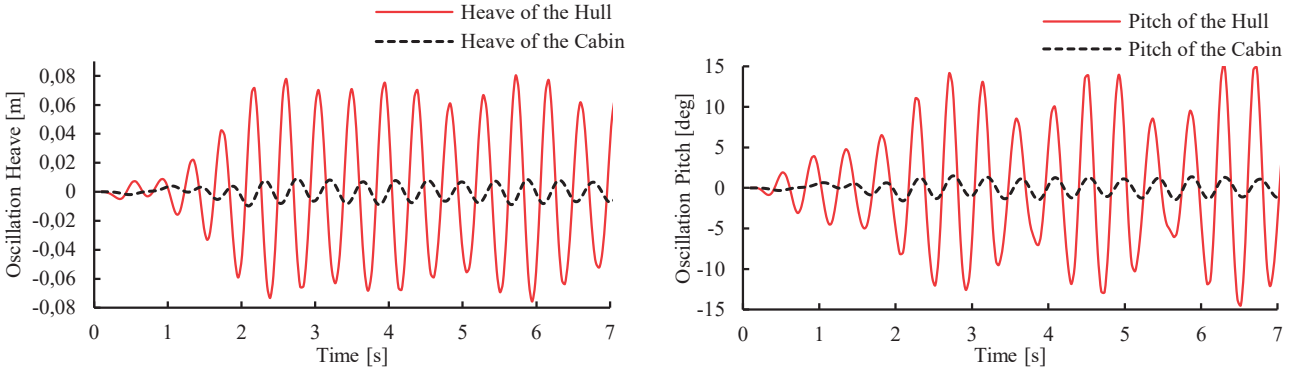

(b) λ/L=2

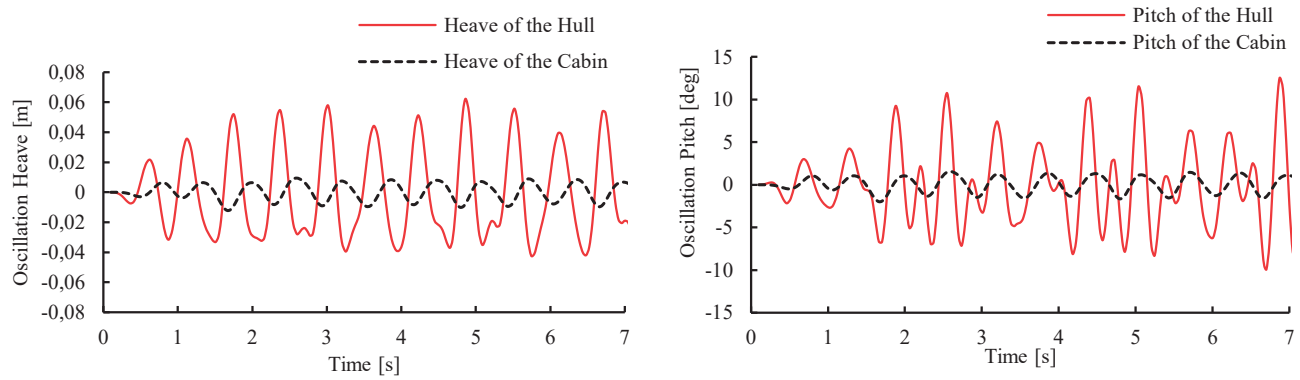

(c) λ/L=3

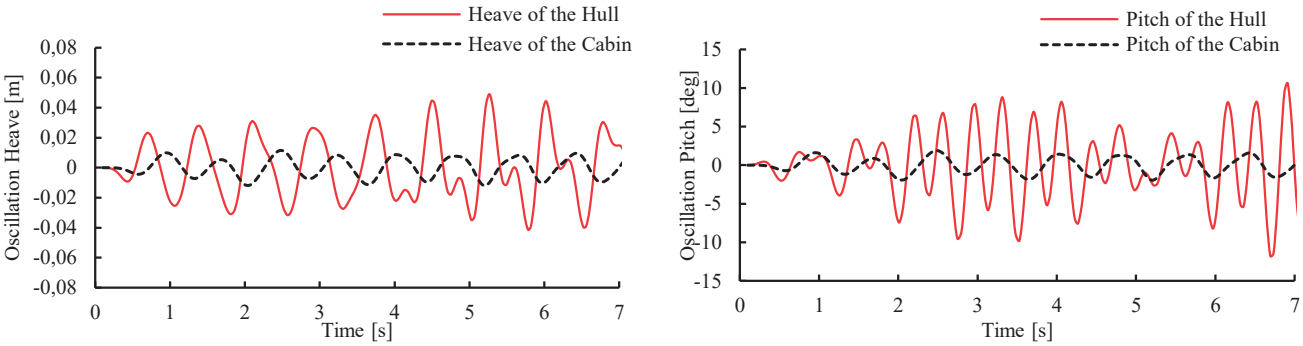

(d) λ/L=4

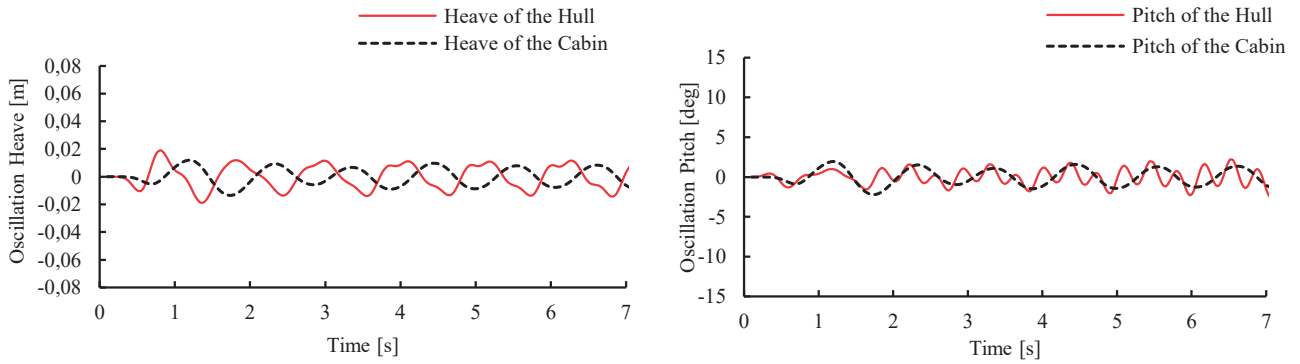

(f) λ/L=6

Fig.13. Time histories of cabin and twin-hull motions of the model boat with cabin (Suspension system) in regular head wave at H/b=0.222 and different wavelengths (Fr=1.2): (left) heave motion, (right) pitch motion

Tab. 6. Main specifications of the suspension system

Parameter	l_1	l_2	K	C_1	C_2
Value	0.36 m	0.36 m	115 N/m	9 N.s/m	9 N.s/m

Tab. 7. Results of cabin motions of the model boat with cabin (Suspension system) in regular head waves at H/b=0.111-0.222 and different λ/L (Fr=1.2)

λ/L	H/b=0.111		H/b=0.222	
	Heave [m]	Pitch [deg]	Heave [m]	Pitch [deg]
1	0.001	0.24	0.001	0.35
2	0.008	1.48	0.018	2.88
3	0.009	1.55	0.018	2.93
4	0.009	1.49	0.019	3.32
6	0.008	1.37	0.017	2.69

DISCUSSION AND COMPARISON

Fig. 14 shows the numerical result of time histories of heave and pitch motions for various models in head waves at two H/b =0.111, 0.222, and λ/L =4. As can be seen from Fig. 14, the suspension system significantly reduces the motion of heave and pitch in the boat cabin, but the Rigid body model has increased the boat's motions compared to the bare hull at this wavelength.

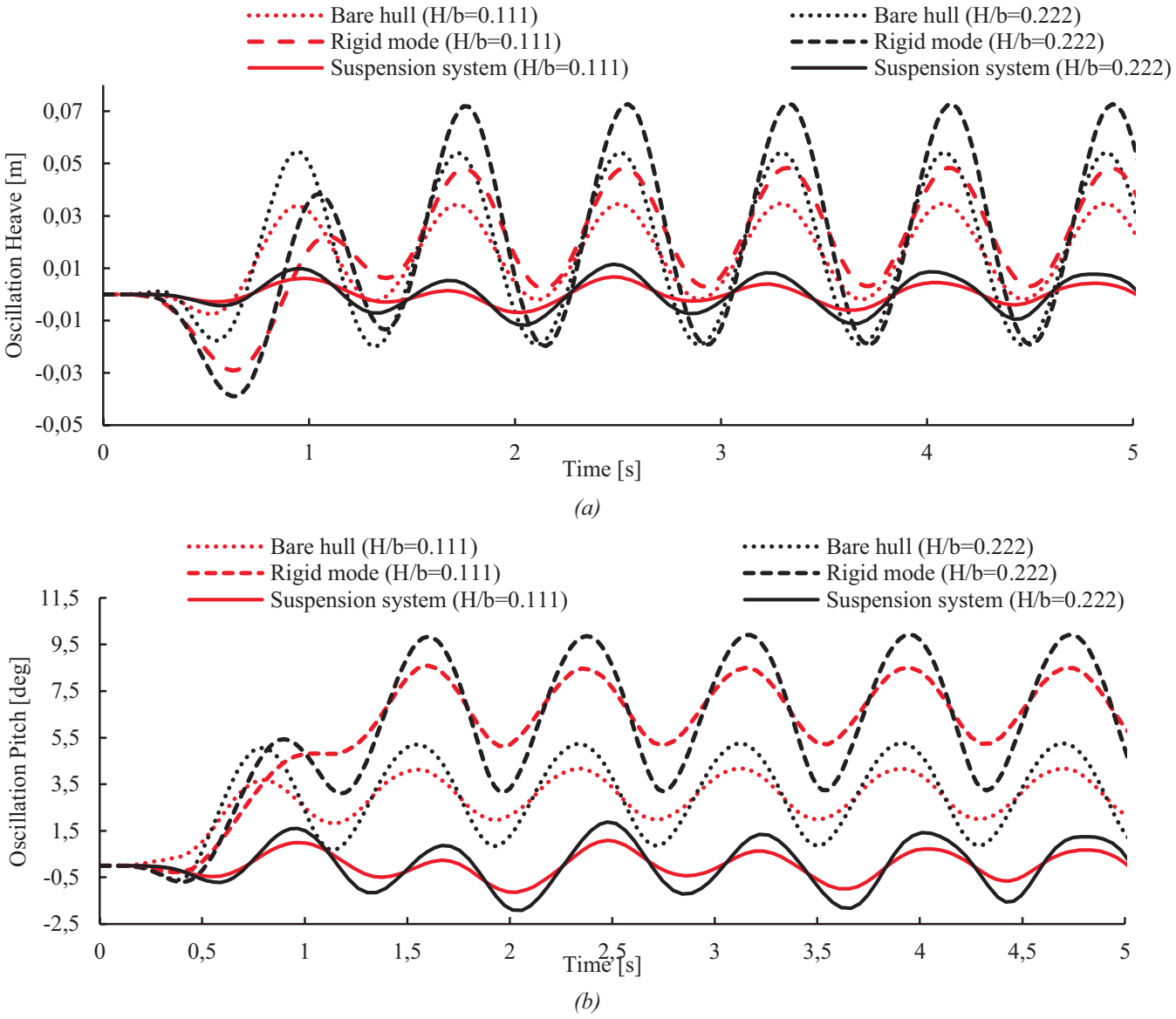

Fig. 14. Comparison of time history of the heave and pitch motions for different models in head waves at two H/b=0.111,0.222 and λ/L=4 (Fr=1.2): (a) heave motion, (b) pitch motion

Figs. 15 and 16 show numerical results of RAOs of heave and pitch motions for models in head waves at two H/b =0.111, 0.222, and various λ/L. It can be seen that RAOs values in all λ/L and both wave heights in the mode with suspension are much lower than in the rigid mode and bare hull. The difference in their values in the high λ/L is very considerable, which is a sign of good boat performance with the cabin in the state with suspension compared to without suspension in heave and pitch motions. Also, compare rigid mode motions with the bare hull; rigid mode reduces motions

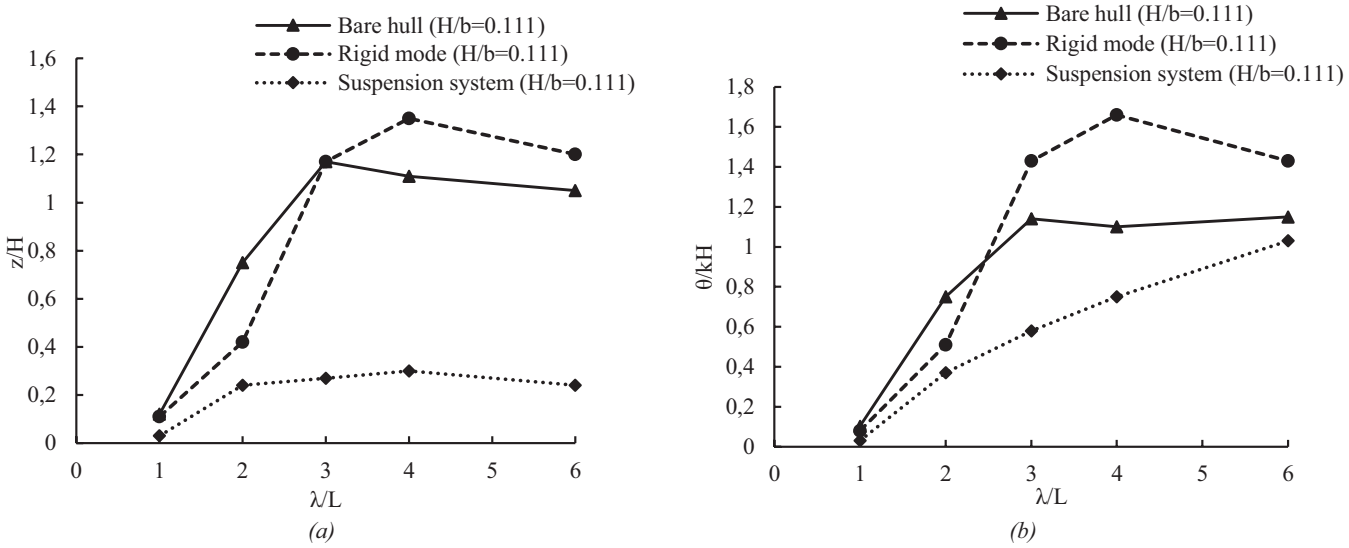

Fig. 15. Comparison of RAOs of the heave and pitch motions for different models in head waves at H/b=0.111and various λ/L (Fr=1.2): (a) heave motion, (b) pitch motion

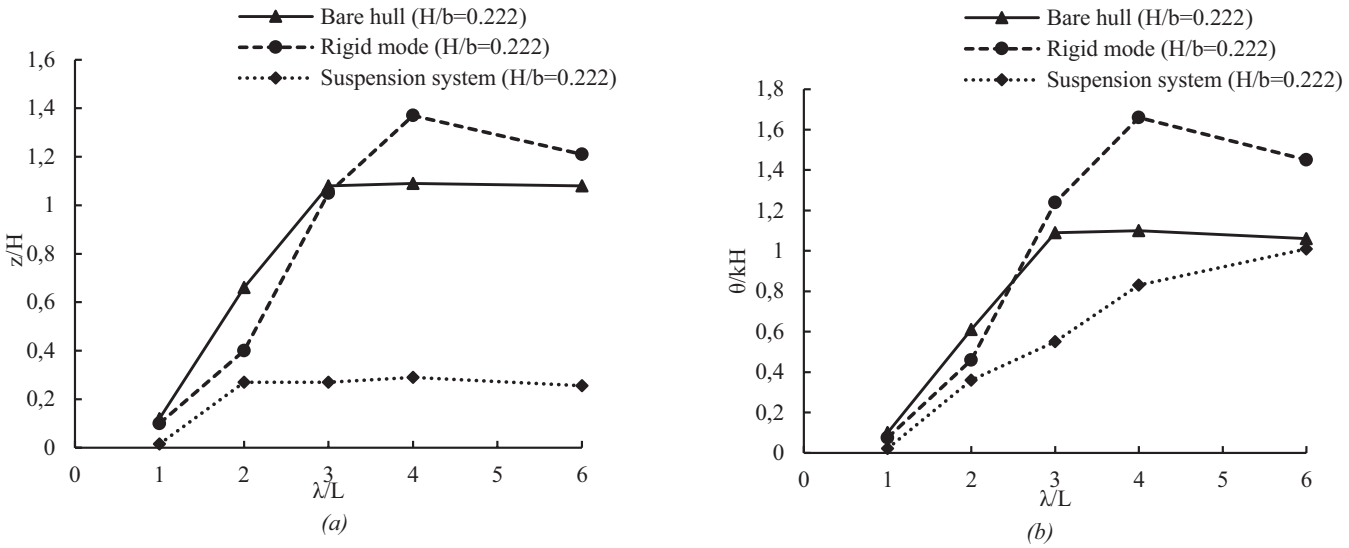

Fig. 16. Comparison of RAOs of the heave and pitch motions for different models in head waves at H/b=0.222 and various λ/L (Fr=1.2): (a) heave motion, (b) pitch motion

CONCLUSIONS

This paper proposes and evaluates a novel concept boat equipped with a suspended cabin and numerical analysis was carried out to investigate motions. The motions of the boat and cabin were investigated, and the effect of the suspension system on cabin motions was evaluated in regular waves. For this purpose, the Fridsma model boat was selected. First, the boat was simulated in STAR-CCM+ software, and the motions were calculated at Froude number 1.2, two wave heights (H/b=0.111, 0.222) and five different wavelengths. The results were compared with Fridsma's experimental tests for validation. The simulation results with less than 10% error rate were considered acceptable.

In the next phase, the cabin is positioned at a set distance on the top of the boat and is joined via a rigid body. The simulation was done in the software at the same Froude number of 1.2, two wave heights (H/b=0.111, 0.222), and different wavelengths. The results showed Rigid mode reduces motions relative to the bare hull only at low wavelengths.

Heave and pitch motions of the cabin were investigated in the final phase for the boat with a suspension system at the same Froude number of 1.2, two wave heights (H/b = 0.111, 0.222) and varied wavelengths. MATLAB software simulated the suspension system between the boat and the cabin. The results showed that the heave and pitch motions of the cabin had been significantly decreased, with heave motions reduced by 32 to 85 percent and pitch motions reduced by 10 to 78 percent at different wavelengths. The maximum

reduction of heave motion in H/b=0.111 and H/b=0.222 was at λ/=1, which was 75% and 85%, respectively. Also, maximum reduction of pitch motion in H/b=0.111 and H/b=0.222 was at λ/L=1, which was 70% and 78%, respectively.

For future work, analyzing the boat equipped with a suspended cabin in 6-DOF needs to be considered. Furthermore, it is also useful to study the optimization of the value of spring stiffness and damper coefficient to reduce the motion of the cabin.

NOMENCLATURE

z	Displacement of the heave of the hull
Z	Displacement of the heave of the cabin
θ	Displacement of the pitch of the hull
Θ	Displacement of the pitch of the cabin
H	Wave height
k	Wave number
λ	Wavelength
Fr	Froude number
V	Velocity of the boat
L	Length of the hull (boat)
b	Breadth of the hull (boat)
h	Height of the hull (boat)
L_c	Length of the cabin
b_c	Breadth of the cabin
h_c	Height of the cabin
m	Mass of the hull
M	Mass of the cabin
i	Moment of inertia of the hull
I	Moment of inertia of the cabin
$X_{Cg,\ hull}$	Longitudinal distance of center of gravity of the hull
$X_{Cg,\ cabin}$	Longitudinal distance of center of gravity of the cabin
$Z_{Cg,\ hull}$	Vertical distance of center of gravity of the hull
$Z_{Cg,\ cabin}$	Vertical distance of center of gravity of the cabin
K	Compression spring constant
C_1	Front damping coefficient
C_2	Rear damping coefficient
E_3	Wave exciting force
E_5	Wave exciting moment
a_{ij}	Added mass
b_{ij}	Damping coefficient
k_{ij}	Stiffness coefficient
l_1	Horizontal distance from front suspension to CG, Cg
l_2	Horizontal distance from rear suspension to CG, Cg
Z'_{cab}	Vertical velocity of the heave of the cabin
θ'_{cab}	Angular velocity of the pitch of the cabin
Z_{fore}	Relative displacement of the front suspension
Z'_{fore}	Relative velocity of the front suspension
Z_{aft}	Relative displacement of the rear suspension
Z'_{aft}	Relative velocity of the rear suspension
Z'_{hull}	Vertical velocity of the heave of the hull
θ'_{hull}	Angular velocity of the pitch of the hull
N	Number of mesh
GCI	Grid Convergence Index

REFERENCE

1. J. Han, D. Kitazawa, T. Kinoshita, T. Maeda, and H. Itakura, 'Experimental investigation on a cabin-suspended catamaran in terms of motion reduction and wave energy harvesting by means of a semi-active motion control system', *Appl. Ocean Res.*, vol. 83, no. February 2018, pp. 88–102, 2019, doi: 10.1016/j.apor.2018.12.003.

2. 'Takahashi, T., Arinaga, S., Ishii, T. Investigation into the technical feasibility of a hi-stable cabin craft (1986) Trans. West-Jpn. Soc. Naval Arch., 72, pp. 213-226.'

3. 'Kihara, K., Hamada, C., Ohnaka, S., Kitamura, T. Development of a 200 passenger hi-stable cabin craft (1991) Trans. West-Jpn. Soc. Naval Arch., 81, pp. 57-69.'

4. A. Kükner and K. Sariöz, 'High speed hull form optimisation for seakeeping', *Adv. Eng. Softw.*, vol. 22, no. 3, pp. 179–189, 1995, doi: 10.1016/0965-9978(95)00016-P.

5. S. M. Cook, P. Couser, and K. Klaka, 'Investigation into wave loads and catamarans', *hydrodyn. High Speed Cr.*, no. November, pp. 24–25, 1999.

6. '"Chenliang Lu, 2010, 'A comfortable boat with suspensions absorbing wave power', Master Thesis, Department of Systems Innovation, School of Engineering, the University of Tokyo."'

7. '"Tsukamoto, Daisuke; 'Basic research on a wave energy absorbing and motion-controlled ship', the University of Tokyo. In Japanese, 2012."'

8. 'V. Marine, http:// www.velodynemarine.com/ (2012). URL http:// www.velodynemarine.com/.'

9. 'N.-C. P. Ltd, http:// www.nauti-craft.com/ (2014). URL http:// www.nauti-craft. com/'.

10. 'Marine Advanced Robotics,https://www.wam-v.com(2005-2021)/.URL https://www.wam-v.com/'.

11. J. F. and K. von E. Manhar R. Dhanak, P. Ananthakrishnan, 'Seakeeping characteristics of a wave-adaptive modular unmanned surface vehicle', *Int. Conf. Ocean. Offshore Arct. Eng.*

12. 'Han, Jialin; Maeda, Teruo; Kinoshita, Takeshi; Kitazawa, Daisuke; 2013a, "Towing test and analysis of an oscillation controlled small ship with wave energy converters", World NAOE Forum 2013 &International Symposium on Marine and Offshore Renewable Energy'.

13. 'Han, Jialin; Maeda, Teruo; Kinoshita, Takeshi; Kitazawa, Daisuke; 2013b, "Research on a motion-controlled ship by harvesting wave energy– based on a semi-active control system", the 6 th East Asia Workshop for Marine Environment and Energy, Qingdao, China'.

14. 'Han, Jialin; Maeda, Teruo; Kinoshita, Takeshi; Kitazawa, Daisuke; "Towing test and motion analysis of a motion-controlled ship- based on an application of skyhook theory", Proceedings of the 12th International Conference on the Stability of Ships and Ocea'.

15. '"CD-Adapco., User guide STAR-CCM+ Version 13.0.6, 2017."'

16. 'HIRT, C. & NICHOLS, B. 1981. Volume of fluid (VOF) method for the dynamics of free boundaries. J. Comput. Phys,, 39 201–225.'

17. 'O.M. Faltinsen, "Hydrodynamics of High-Speed Marine Vehicles, Ch. 9- Planing vessles", Cambridge University Press, 2005.'

18. G. Fridsma, 'A systematic study of the rough-water performance of planing boats', Stevens Inst Of Tech Hoboken Nj Davidson Lab, 1969.

19. 'ITTC. Practical Guidelines for Ship CFD Application. ITTC–Recommended Procedures and Guidelines, 2011b. ITTC.'

20. O. F. Sukas, O. K. Kinaci, F. Cakici, and M. K. Gokce, 'Hydrodynamic assessment of planing hulls using overset grids', *Phys. Procedia*, vol. 65, pp. 35–46, 2017, doi: 10.1016/j.apor.2017.03.015.

21. H. Ghassemi, M. Kamarlouei, and S. Taj Golah Veysi, 'A hydrodynamic methodology and cfd analysis for performance prediction of stepped planing hulls', *Polish Marit. Res,* vol. 22, no. 2, pp. 23–31, 2015.

22. A. Nadery and H. Ghassemi, 'Numerical investigation of the hydrodynamic performance of the propeller behind the ship with and without WED', *Polish Marit. Res.*, vol. 27, no. 4, pp. 50–59, 2020, doi: 10.2478/pomr-2020-0065.

23. I. B. Celik, U. Ghia, P. J. Roache, C. J. Freitas, H. Coleman, and P. E. Raad, 'Procedure for estimation and reporting of uncertainty due to discretization in CFD applications', *J. Fluids Eng.*, vol. 130, no. 7, pp. 078001–078004, 2008, doi: 10.1115/1.2960953.

CONTACT WITH THE AUTHORS

Hassan Bahrami
hassan.bahrami1996@gmail.com

Hassan Ghassemi
e-mail: gasemi@aut.ac.ir

Amirkabir University of Technology
Hafez, 123123 Tehran,
Iran